

Tunneling and hopping conduction in Langmuir-Blodgett thin films of poly(3-hexylthiophene)

E. Punkka* and M. F. Rubner

Department of Materials Science and Engineering, Massachusetts Institute of Technology, Cambridge, Massachusetts 02139

J. D. Hettinger and J. S. Brooks

Physics Department, Boston University, Boston, Massachusetts 02215

S. T. Hannahs

Francis Bitter National Magnetic Laboratory, Massachusetts Institute of Technology, Cambridge, Massachusetts 02139

(Received 19 October 1990)

The electrical conductivity and field-effect mobility of undoped and NOPF₆-doped Langmuir-Blodgett thin films of poly(3-hexylthiophene) have been measured as a function of temperature, electric field, and film thickness. These properties are compared with those of free-standing films. In undoped samples the conductivity is best described by variable-range hopping, whereas in the doped and dedoped states the model of charging-energy-limited tunneling between conducting islands is applicable. The data indicate metallic charge carrier densities within the conducting islands in the highly doped state. At electric fields close to the dielectric breakdown, a possible onset to Fowler-Nordheim tunneling is observed. As the samples become dedoped, the electrical properties indicate an increase in the average size of conducting islands, which are suggested to consist of polymer backbones separated by the alkyl side chains of neighboring molecules.

I. INTRODUCTION

The mechanisms of electrical conduction in inherently conducting polymers are still a matter of controversy. The concept of solitons and polarons acting as charge carriers has been widely accepted, but the physical processes involved in their motion through the material remain unsolved to some extent. Conducting polymers are usually highly disordered materials with considerable amounts of impurities. The electrical properties reflect the structure of the polymer, which depends on the method of preparation and processing. The characterization and modeling of electrical conduction is thus a difficult task and comparisons of experimental results between research groups can easily lead to wrong conclusions if the materials are not similar by structure.

The experimental studies on conducting polymers have shown that the conductivity mechanism is dependent on the degree of doping. Doping, on the other hand, is known to alter the structure of conjugated polymers. Tunneling and hopping models have usually been used in explaining the conductivity behavior. For example, in polyacetylene, the most studied conducting polymer, the observed electrical properties have been related to the theories of variable-range hopping,¹ charging-energy-limited tunneling,² thermal fluctuation-induced tunneling,^{3,4} intersoliton hopping,⁵ and bipolaron hopping,⁶ depending on the degree of doping or other factors. These models have been used in describing the charge transport in other inherently conducting polymers too.

We are currently studying the electrical properties of thin films of conducting polymers prepared by the Langmuir-Blodgett (LB) technique. The recent progress in this field⁷ makes it possible to manipulate poly(3-

alkylthiophenes) into well-defined layered structures with controllable thickness. They can be subsequently doped by chemical oxidation, which makes the film conductive. The controllability of LB manipulation may be used in examining the effect of structure on the electrical properties and the good reproducibility of the film structure offers a possibility for detailed studies on the conduction mechanisms in these materials. In this paper we report the results of a series of detailed electrical measurements in undoped and NOPF₆-doped LB films and free-standing films of poly(3-hexylthiophene) (PHT). The measurements include the temperature, electric field, thickness, and pressure dependences of the conductivity, as well as the thickness and temperature dependences of the field-effect mobility. The applicabilities of the models of variable-range hopping and charging-energy-limited tunneling are tested, and the conductivity behavior is compared to that of free-standing films of PHT.

II. EXPERIMENT

Poly(3-hexylthiophene) was prepared by the direct oxidation of 3-hexylthiophene monomer by FeCl₃ as described elsewhere.⁸ Free-standing films (thickness 30–50 μm) were cast from chloroform solution. The molecular weight of the polymer was $M_w = 75\,700$ g/mol and $M_n = 18\,000$ g/mol. Elemental analysis was performed by Schwarzkopf Microanalytical Laboratory, Inc. The results showed an Fe impurity concentration of about 7×10^{18} cm⁻³ in the undoped polymer. Weight uptake measurements indicate dopant concentrations of about 20 mol % in the NOPF₆- and FeCl₃-doped polymers.

LB deposition was performed by mixing PHT and surface active 3-octadecanoylpyrrole (3ODOP) (molar ratio

5:1) in a chloroform solution and spreading it onto a purified subphase of water in a Lauda film balance. By using 3-octadecanoylpyrrole, the films are free from Cd ions, unlike in films where stearic acid is used as the surface active element and CdCl_2 is needed in the subphase. This is especially important in electrical measurements with a two-point configuration of electrodes. The number of layers ranged from 3 to 25, which corresponds to film thicknesses from 150 to 1250 Å according to ellipsometric measurements.

Doping was carried out chemically with NOPF_6 in acetonitrile and FeCl_3 in nitromethane. The doping time was 90 min for free-standing films and 10 min for LB films. The dopant concentration in solution was 0.5 g/l for NOPF_6 (0.1 g/l in the case of the LB films) and 10 g/l for FeCl_3 .

dc conductivity was measured in vacuum in a cryostat over a temperature range of 4.3–300 K. Free-standing films were contacted with carbon paste, which forms an Ohmic contact to PHT and measurements were performed by the standard four-point method except in the case of the electric-field dependence in which two points were used. Langmuir-Blodgett films were deposited on a specially designed field-effect transistor (FET) electrode configuration⁹ (Fig. 1), which allowed the simultaneous measurements of conductivity and field-effect mobility. Gold electrodes (100 Å Cr plus 200 Å Au) deposited on silicon oxide (3000 Å thermally grown on an *n*-type Si wafer) were interdigitated having a channel width of 8 or 4 cm, but a length of only 5 μm. Gold also forms an Ohmic contact to PHT.

The electric-field dependence of the conductivity was measured by applying a dc voltage across the electrodes. In some cases the behavior was checked with a pulse generator at a frequency of 10 Hz and a pulse width determined by the *RC* constant of the load. However, no difference in conductivity was observed.

The pressure-dependent conductivity of free-standing films of PHT doped with FeCl_3 was measured up to 1.7 GPa in a hydrostatic BeCu pressure clamp of standard design¹⁰ at room temperature. The current and voltage leads for four terminal conductivity measurements were 25-μm gold wires attached to the film with carbon paste. The sample was then placed in a Teflon bucket filled with a perfluorocarbon pressurizing fluid. The bucket and

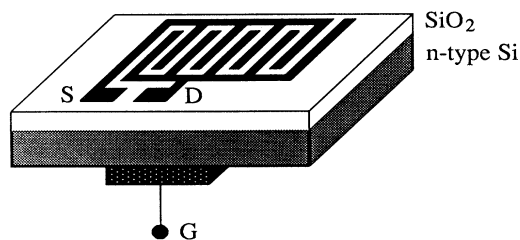


FIG. 1. Field-effect transistor electrode configuration. The actual number of interdigitated gold electrode fingers is 20 or 40, giving a channel width of 4 or 8 cm. The channel length is 5 μm. The LB films are deposited on top of the electrodes.

BeCu cap with an epoxy electrical feedthrough were compressed in a BeCu cylinder between two tungsten carbide pistons with a hydraulic press. The pressure was monitored by a strain gauge on the press, and the voltage was recorded as the pressure was varied. The current through the sample was kept less than 1 mA at all times. The measurements were repeatable over several cycles of the clamping pressure. Any hysteresis in the measurements seemed to be due to friction of the pistons against the walls, which would cause a force differential across the piston. This hysteresis was reduced to almost zero after several cycles of the pressure.

III. RESULTS

The LB film samples used in this study had thicknesses of 3, 11, 21, and 25 layers. We use terms undoped, doped, dedoped, and redoped in describing the sample history. Undoped means the as-deposited films. Doped refers to measurements made immediately after doping. After doping the conductivity decreases and the sample becomes dedoped. In dedoped samples we may distinguish a moderately dedoped state when the room-temperature conductivity is above 10^{-4} S/cm. If a dedoped sample is doped, it will be called redoped. The temperature and the electric-field dependence of the conductivity were measured in all samples. Detailed electric-field dependence measurements were performed in a 25-layer sample which was dedoped by venting the sample chamber and letting the conductivity decrease at room temperature in laboratory air. The measurements of the moderately dedoped and (more fully) dedoped states were then made after 12 and 27 days from doping, respectively. The temperature dependence of the field-effect mobility was measured in samples of 3 and 21 layers. The effect of redoping was studied in an 11-layer sample. The measurements of the undoped material were performed in a sample of 25 layers. Free-standing films were studied only in the doped state.

A. Field-effect measurements

Due to the large parallel bulk conductance of the LB film, the polymer transistors studied here are normally-on devices with nonlinear, nonsaturating *I-V* characteristics at high biases. Figure 2 shows the effect of gate voltage V_G on drain-source current I_{DS} in a three-layer sample after dedoping. A negative gate voltage accumulates *p*-type charge carriers at the polymer- SiO_2 interface, whereas a positive gate voltage depletes the charge carriers away from the conduction channel. No saturation current can be observed at higher biases, which is caused by a non-Ohmic conduction at high electric fields. Undoped polymer transistors can be driven to the saturation region¹¹ and they can be made normally-off devices if the bulk resistance is increased for example by a heat treatment or by reducing the thickness of the film. We did not observe any saturation in I_{DS} in doped samples even after prolonged dedoping. The field-effect mobility μ in the linear region can be calculated by measuring the channel conductance g_d at low bias V_{DS} and using the well-known equation¹²

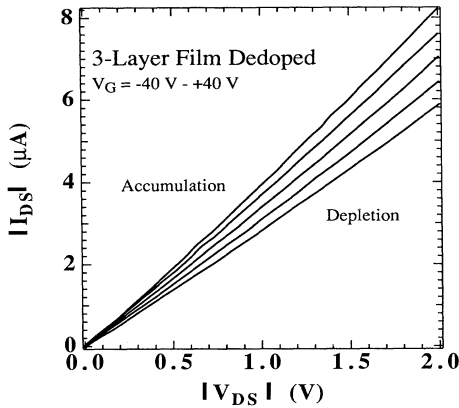


FIG. 2. Current-voltage characteristics of a dedoped 3-layer LB-FET in the linear region. The gate voltage was varied from -40 to $+40$ V with steps of 20 V.

$$g_d = \frac{\Delta I_D}{\Delta V_{DS}} = \frac{w}{L} \mu C_{ox} (V_G - V_T) \quad (1)$$

as $V_{DS} \rightarrow 0$. V_T is the threshold voltage and C_{ox} the oxide capacitance. w and L are the channel width and length, respectively.

Figure 3 shows the conductivity and the field-effect mobility measured as a function of the film thickness before and after doping with NOPF₆. The samples were deposited on the same substrate by adjusting the depth of the dip of the substrate wafer in the LB trough. There were about eight transistors with each thickness. The gate voltage did not have any effect on the channel conductance immediately after doping. This was probably caused by the film being lifted off the SiO₂ interface by the solvent during doping. The field-effect measurements of the doped state were thus performed after storing the samples for three days in nitrogen. By that time the conductivity had decreased by a factor of about 2. As can be

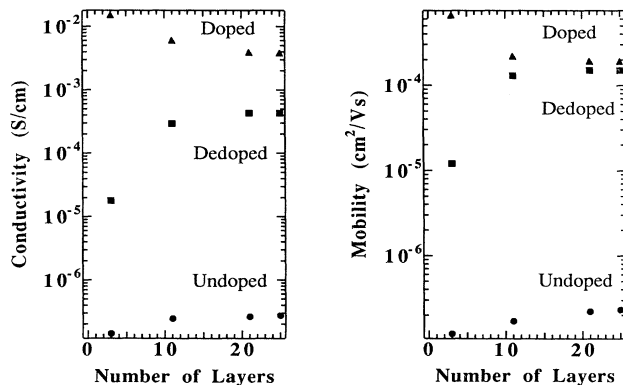


FIG. 3. Conductivity and the field-effect mobility before and after doping with NOPF₆ as a function of the number of layers deposited.

seen in Fig. 3, doping increased the conductivity by five orders of magnitude and the mobility only an order of magnitude less, which shows that the conductivity increase is mainly due to a change in mobility. The increase is fairly independent of thickness within the experimental error, except in the thinnest sample of three layers. After doping the conductivity starts degrading. Dedoping proceeds much faster in air as the PF₆⁻ molecules react with moisture and become inactive. In the thinnest sample the decrease in conductivity is due to a decrease in both the mobility and the active dopant concentration, whereas in thicker films the mobility changes more slowly and is not very much thickness dependent.

The temperature dependence of the field-effect mobility in a dedoped three-layer sample is shown in Fig. 4. The data fit best a $\log_{10} \mu \propto T^{-0.5}$ dependence in the accumulation mode, but the depletion mobility behaves more according to a $\log_{10} \mu \propto T^{-1}$ law and vanished completely below 150 K. When the measurement was repeated in a thicker film of 21 layers and at a higher doping level, the relative difference between the accumulation and the depletion mobilities was not as great as in Fig. 4, but the behavior was qualitatively the same. The accumulation mobility has the same temperature dependence as the conductivity (see Fig. 5), which will be discussed in Sec. III B. This gives also the carrier concentration $\sigma/e\mu$ the same temperature dependence, which, however, is relatively small, as seen in Fig. 5.

B. Conductivity in doped LB films

The temperature dependence of the conductivity in doped and dedoped samples was always found to obey well the exponential law

$$\sigma = \sigma_0 e^{-(T_0/T)^{1/2}} \quad (2)$$

Figure 6 shows $\sigma(T)$ measured in a 25-layer sample at different dedoping levels. At high conductivities (above 0.01 S/cm) the sample resistance became comparable to the series resistance formed by the cryostat measurement

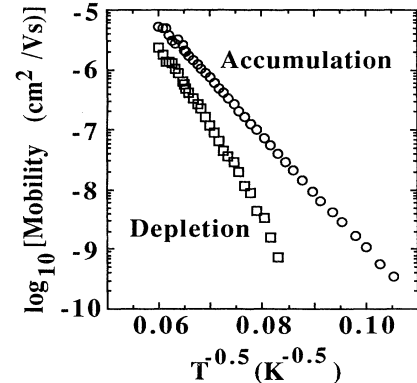


FIG. 4. Field-effect mobility in accumulation ($V_G = -30$ V) and depletion ($V_G = +30$ V) as a function of temperature in a dedoped 3-layer LB FET.

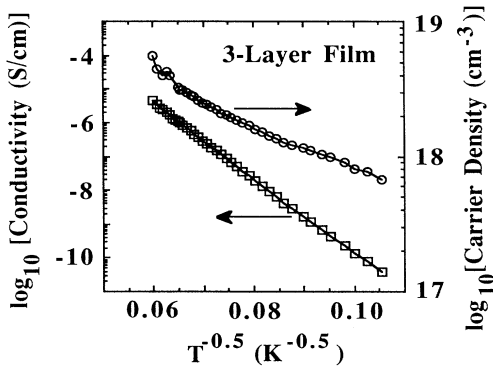


FIG. 5. Conductivity and the charge-carrier concentration ($\sigma/e\mu$) as a function of temperature in a dedoped 3-layer LB FET.

leads and the contact resistance. This is due to the large channel width and the small channel length of our electrode configuration. Thus the conductivity was not measurable in this sample at high temperatures. Extrapolating the slope in Fig. 6 gives a room-temperature conductivity of 0.1 S/cm. After dedoping the activation energy increases (see Table I), but the temperature dependence can still be fitted to Eq. (2) in an excellent way.

The behavior of Eq. (2) is predicted by various models, such as one-dimensional variable-range hopping,¹³ variable-range hopping with a quadratic density of states:¹⁴ $N(E) \propto (E - E_F)^2$, or charging-energy-limited tunneling between metallic islands.¹⁵ It is necessary to perform other measurements in order to distinguish between these models. Figure 7 shows the electric-field dependence of the resistivity at high fields and at a low temperature in the same 25-layer sample of Fig. 6. According to the model of the charging-energy-limited tunneling the resistivity should then behave exponentially

$$R = R_0 e^{E_0/E}. \quad (3)$$

This is exactly what is observed in Fig. 7 with the slope increasing as the sample becomes dedoped. Another proof of the applicability of this model is shown in Fig. 8 where the electric-field dependence of the conductivity has been measured at different temperatures. The data have been fitted to the complete field and temperature

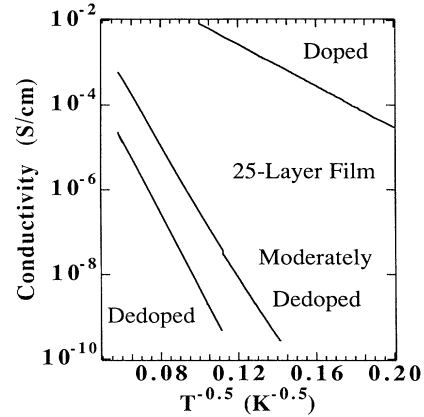


FIG. 6. Temperature dependence of the conductivity at different states of dedoping in a 25-layer sample.

dependence of Sheng and Abeles¹⁵

$$\sigma = \sigma_\infty e^{-1/E^*} \times \int_{-1/E^*}^{\infty} dZ Z \frac{e^{-Z}}{1 - \exp\{-ZE^*/[(Z + 1/E^*)T^*]\}}, \quad (4)$$

where $E^* = E/E_0$ and $T^* = 4T/T_0$. Z is an integration variable dependent on the electric field, the charging energy, and the tunneling barrier parameters. E_0 and T_0 are determined from Figs. 6 and 7, respectively (see Table I), which leaves only one adjustable parameter σ_∞ determining the amplitude of the function of Eq. (4). E_0 and T_0 determine the shape of the curve, and as shown in Fig. 8(a), a satisfactorily good fit can be obtained especially at high fields by using these values obtained from the low field $\sigma(T)$ and the low temperature $R(E)$. As the sample becomes dedoped we need to adjust T^* in order to make good fits in Figs. 8(b) and 8(c). The tendency is that Eq. (4) gives then slightly too strong a curvature if the measured value of T_0 is used. At low temperatures Eq. (4) is very insensitive to changes in T_0 and therefore a fairly large increase of T^* is needed in order to improve the fit.

Table I also shows the parameters measured in an 11-layer sample after three cycles of doping and dedoping. Redoping increases the conductivity, but it does not rise

TABLE I. Parameters of a doped, moderately dedoped, and dedoped 25-layer film, and a redoped and dedoped 11-layer film.

Sample	σ_{r1} (S/cm)	σ_0 (S/cm)	kT_0 (eV)	σ_∞ (S/cm)	E_0 (MV/cm)	w' (Å)
doped	0.1	3	0.29	2×10^{-2}	0.17	42
moderately dedoped	6×10^{-4}	20	2.7	1×10^{-3}	1.1	61
dedoped	2×10^{-5}	2	3.5	3×10^{-4}	1.4	63
redoped and dedoped	3×10^{-6}	25	6.6	3×10^{-6}	1.6	106

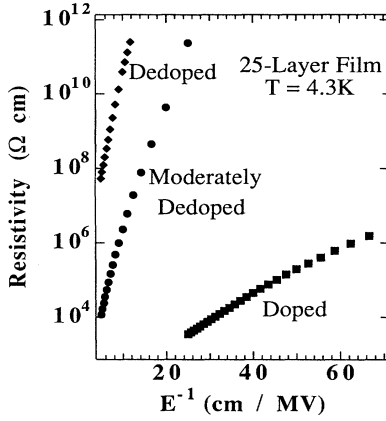


FIG. 7. High-electric-field dependence of the resistivity at different states of dedoping in a 25-layer sample at 4.3 K.

as high as in the first doping; usually the maximum conductivity is one or two orders of magnitude smaller. The temperature and the electric-field dependences of the conductivity still agreed equally well with the theory of charging-energy-limited tunneling. The breakdown field was studied in this redoped and dedoped sample of 11 layers at 4.3 K. The data are shown in Fig. 9. Some deviating behavior from the slope (E_0) of Table I was observed in the field dependence of resistance starting around 0.3 MV/cm. The resistivity seemed to have transition points after which it decreased according to Eq. (3), but with an increasingly steeper slope. The current density was 11 A/cm² right before the breakdown, which occurred at an electric-field strength of 0.52 MV/cm. The breakdown increased the current by several orders of magnitude and the sample temperature started rising. After the breakdown the sample remained in a highly conducting state, which suggests that carbonization of the film had occurred. The tunneling behavior before the breakdown will be discussed later in this paper.

C. Conductivity in undoped LB films

The temperature dependence of the conductivity in an undoped 25-layer sample was best fitted to the model of three-dimensional variable range hopping¹²

$$\sigma = \sigma_1 e^{-(T_1/T)^{1/4}} \quad (5)$$

at low bias. Figure 10 shows also the effect of electric field on the behavior of the conductivity. The data have been fitted to the form of the variable-range hopping model developed by Apsley and Hughes¹⁶

$$\sigma = \frac{a^2 N e^2 \nu}{2} \left[\frac{a^3 N \pi k T}{24} \right]^{-1/4} \times \exp\{-[48/a^3 N \pi k T (P + Q)]^{1/4}\}, \quad (6)$$

where

$$P = \frac{1 + \beta/2}{(1 + \beta)^2}, \quad Q = 1 + \frac{3\beta}{2}, \quad \beta = \frac{aEe}{2kT}.$$

The advantage of varying the electric field is that the density of states at the Fermi level $N(E_F)$ and the localization length a can be fitted separately. The best fit was obtained with $N(E_F) = 4.7 \times 10^{16} \text{ eV}^{-1} \text{ cm}^{-3}$ and $a = 9.9 \text{ \AA}$. As in inorganic amorphous semiconductors¹⁷ the localization length needs to be corrected as the electric field changes. In this case, a needed to be increased to 11.4

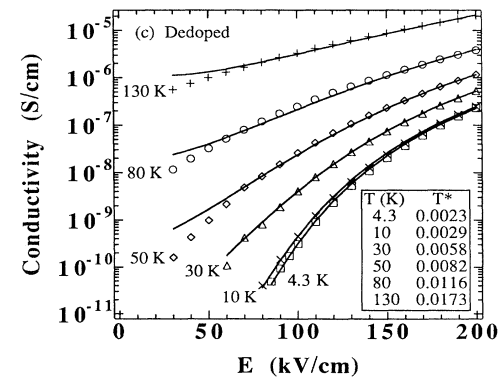
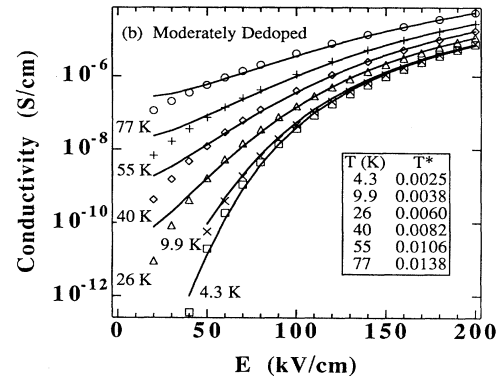
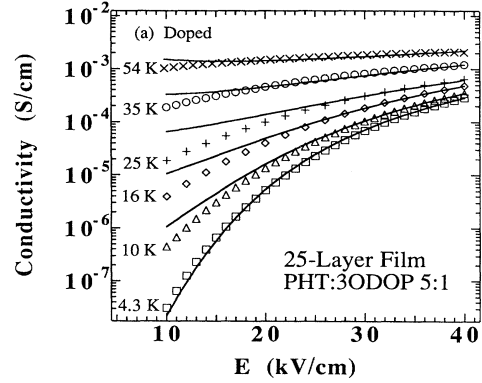


FIG. 8. Electric-field dependence of the conductivity fitted to the model of charging-energy-limited tunneling in a 25-layer sample (a) in the doped state, (b) in the moderately dedoped state, and (c) in the dedoped state. In (b) and (c) the parameter T^* has been adjusted at each temperature (see the tabulated values) in order to make satisfactory fits.

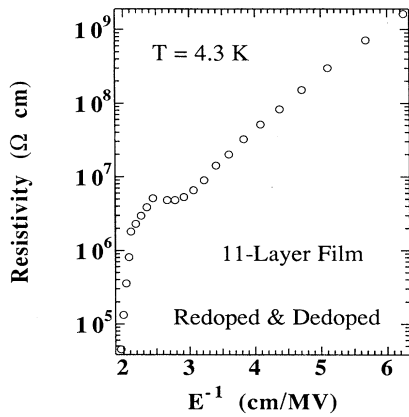


FIG. 9. Behavior of the resistivity close to the dielectric breakdown field in a redoped and dedoped (three cycles of doping and dedoping) 11-layer sample at 4.3 K.

and 12.2 Å as the electric field increased to 60 and 160 kV/cm, respectively. Another feature typical of applying variable-range hopping models is the problem of the pre-factor in Eq. (6), which gives unphysically high jump rates, $3.9 \times 10^{30} \text{ s}^{-1}$ in our case. The data fit the model in a wide temperature range. Notice the kink in the curve of 160 kV/cm at 140 K above which temperature the data start deviating from the theoretical values. These kinds of transitions can sometimes be seen in $\sigma(T)$ curves in both doped and undoped samples (see the data of the moderately dedoped sample in Fig. 6). They occur unexpectedly and usually in an irreproducible way. It is possible that at these transition points the charge carriers find new hopping or tunneling routes, which have different transfer characteristics.

D. Conductivity in doped free-standing films

In order to reveal if the ordered structure of the LB films has any effect on the charge-transport mechanism,

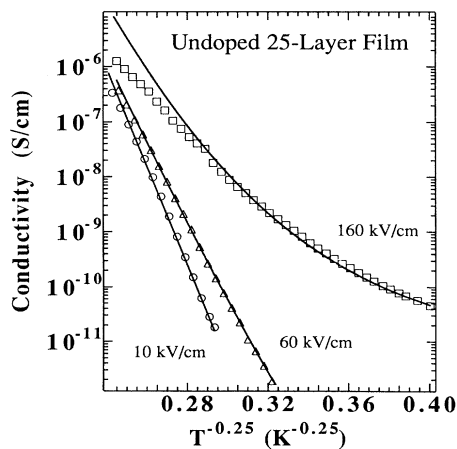


FIG. 10. Temperature dependence of the conductivity at different electric-field strengths in an undoped 25-layer sample.

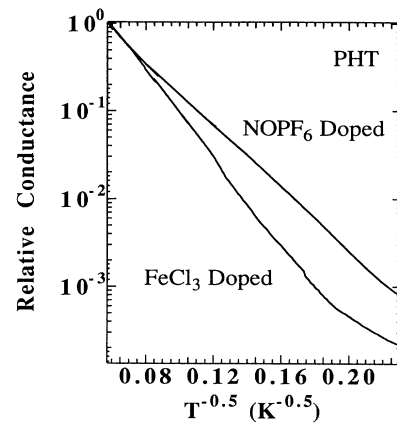


FIG. 11. Temperature dependence of the relative conductance in free-standing films of PHT doped with NOPF₆ or FeCl₃.

the temperature dependence of the conductivity was measured in free-standing films of doped poly(3-hexylthiophene). Figure 11 shows the behavior of $\sigma(T)$ in samples doped with NOPF₆ and FeCl₃. In both cases the best fit was obtained with Eq. (2) as in doped LB films of the same material. The tendency to saturating conductivity at low temperatures (below 30 K) is due to the non-Ohmic behavior of the resistance. This can be seen more clearly in Fig. 12 where the resistance was measured with a two-point electrode configuration. The contacts were made with carbon paste as close to each other as possible. The electrode distance was of the order of 100 μm, but it was impossible to determine it accurately. Thus the electric-field strength is not known in this case. However, the qualitative behavior can be seen to approach the relation of Eq. (3).

It is not possible to use the electrode array structure of field-effect transistors in measurements of free-standing films and therefore the comparatively larger electrode distance prevented us from studying and comparing the

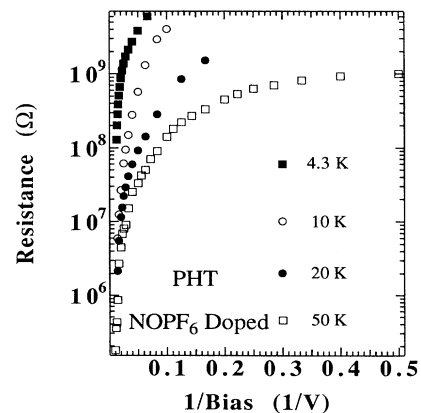


FIG. 12. Bias voltage dependence of the sample resistance at different temperatures in a free-standing film of PHT doped with NOPF₆.

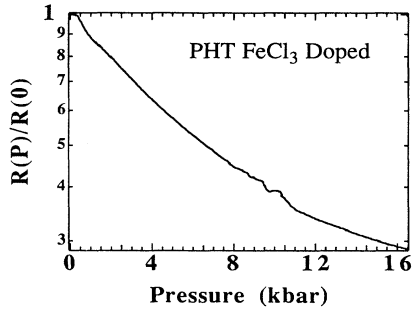


FIG. 13. Relative sample resistance as a function of pressure at room temperature in a free-standing film of PHT doped with FeCl_3 .

high-field conductivity more closely. The pressure dependence was measured instead as shown in Fig. 13. The resistance decreases with increasing pressure as expected if the tunneling barrier width between the conducting islands is reduced. Note that the vertical axis is in a logarithmic scale.

IV. DISCUSSION

A. Undoped LB films

The observed $\log_{10}\sigma \propto T^{-1/4}$ behavior in the undoped sample indicates that the dominant charge-transport mechanism is variable-range hopping. It also means that the density of states is flat, since other densities of states would produce different dependences. The functional form of the electric-field dependence, on the other hand, is still a matter of controversy. We have used the approach of Apsley and Hughes¹⁶ which predicts a $\log_{10}\sigma \propto E^2$ behavior. Pollak and Riess¹⁸ utilized directed percolation and arrived at a linear field dependence of $\log_{10}\sigma$. In both cases there is experimental data supporting the theories. Further work on the directed percolation¹⁹ has given also a $\log_{10}\sigma \propto E^2$ behavior depending on the types of approximations made.

The parameters a , $N(E_F)$, and ν extracted from the field and temperature dependence of conductivity are comparable to the values measured by Yoffe and Phillips¹⁷ in amorphous P and As. In *a*-P they get $a = 10 \text{ \AA}$, $N(E_F) = 5.2 \times 10^{16} \text{ eV}^{-1} \text{ cm}^{-3}$, and $\nu = 7.5 \times 10^{29} \text{ s}^{-1}$, which are very close to the values obtained in this study. However, instead of having to increase the value of a , they had to decrease it in order to maintain a good fit at high fields. This means that in our case the model underestimates the strength of the dependence of the conductivity on electric field, unlike in amorphous inorganic semiconductors. ν is larger than the optical-phonon frequency ($\nu_{\text{ph}} \approx 10^{13} \text{ s}^{-1}$) by a factor of 10^{17} . These features show that the simple model of variable range hopping is not correct, although it can explain many of the main properties of the data.

Knowing a and $N(E_F)$, it is possible to determine the average hopping distance r and the average hopping energy W ,

$$r = \left(\frac{9a}{8\pi kTN(E_F)} \right)^{1/4}, \quad (7)$$

$$W = \frac{3}{4\pi r^3 N(E_F)}, \quad (8)$$

according to Mott's definitions¹³ (Apsley and Hughes used a parameter called range which is the sum of reduced r and W). Substituting a and $N(E_F)$ into Eqs. (7) and (8) gives $r(300 \text{ K}) = 230 \text{ \AA}$ and $W = 0.41 \text{ eV}$. These values are high manifesting the high resistivity of the material. We can then also test the suggestion of Colson and Nagels²⁰ for the jump frequency $\nu \exp(-2R/a) \leq \nu_{\text{ph}}$, which indeed predicts that a hopping distance greater than 200 \AA is expected, if $a = 10 \text{ \AA}$ and $\nu = 10^{30} \text{ s}^{-1}$. With hopping lengths this long we would expect to see a strong thickness dependence of the conductivity in the thinnest films. As shown in Fig. 3, there is a decrease in conductivity with a decreasing number of layers in the undoped state, but the magnitude of the effect is smaller than in a previously reported study of a LB FET of poly(3-hexylthiophene).²¹ This suggests that the charge-carrier hopping length increases more slowly than predicted by percolation models as the two-dimensional hopping regime is approached.

The charge carriers in the undoped materials are caused by synthesis-induced impurities which act as dopants. In this material the impurities are FeCl_3 molecules or other products which are used in the polymerization of poly(3-hexylthiophene). If we assume that hopping occurs between polarons or bipolarons electrostatically bound to dopant molecules the dopant concentration can be estimated to be $3/4\pi r^3$, which gives $2 \times 10^{16} \text{ cm}^{-3}$. This would be the concentration of active dopants or the density of the dopants acting as hopping sites. The estimate is very rough and it would be more justified in the case of nearest-neighbor hopping, whereas in variable-range hopping it can be regarded as the lower limit for the dopant concentration. The value is much less than the total Fe concentration in pure PHT determined by elemental analysis, but it is very close to the dopant concentrations obtained from spin cast PHT Schottky barriers by capacitance-voltage measurements.²² Our own *C-V* measurements²³ probe only the outermost layers and give higher dopant concentrations, of the order of $10^{17} - 10^{18} \text{ cm}^{-3}$, for LB films of PHT. This is due to the fact that in thin films the dopant concentration is much higher near the interface.^{23,24} The value is also over two orders of magnitude smaller than the carrier concentration calculated with the conductivity and the field-effect mobility values of the undoped state in Fig. 3. These concentrations need not be the same, of course, since the application of a gate voltage can create new polarons or bipolarons to the polymer- SiO_2 interface.

With the speculations of polaron hopping we are moving closer to the intersoliton hopping model proposed by Kivelson.²⁵ According to this model the conductivity should vary as $\sigma(T) \propto T^n$. It has been successfully applied to lightly doped *trans*-poly(acetylene) (Ref. 26) and poly(paraphenylene) (Ref. 27) and it could in principle be used here too because a $\log_{10}\sigma - \log_{10}T$ plot of our data

gives a reasonably good linear behavior at a low electric field. A value of $n = 14.3$ can be determined from the slope. However, the intersoliton model lacks an expression for the electric-field dependence and the variable-range hopping model explains our data over a wide temperature range. The choice of variable-range hopping is also supported by the similarity of the data to the corresponding measurements made in inorganic disordered systems, where similar interpolyronic conduction is unlikely to exist. Frequency²⁸ or pressure²⁶ dependence of conductivity could probably determine the applicabilities of these two models.

B. Doped LB films

Doping LB films with NOPF₆ results in a change in charge-transport properties. As shown in Fig. 3 the conductivity increase is caused by a dramatic change in mobility. On the other hand, as the sample becomes dedoped the conductivity decreases mainly because of a drop in charge carrier concentration. The temperature dependence of the conductivity fits the $\log_{10}\sigma \propto T^{-1/2}$ dependence in an excellent way and the electric-field dependence of the resistivity resembles closely that of granular metals.¹⁵ The results strongly indicate that highly conducting islands are formed. It is not clear whether the charge-carrier tunneling between these islands occurs, for example, through undoped polymer segments, polymer side chains or free space. The LB films also contain insulating surface active 3-octadecanoylpyrrole molecules, which, however, are soluble in acetonitrile and are at least partly washed away during doping. The process of LB film deposition supposedly forms a homogeneous blend of 3ODOP and PHT, and the subsequent doping and removing of 3ODOP is then believed to result in a homogeneous mixture of highly conducting PHT or aggregates of PHT molecules. In this case, the layered structure of the LB films disappears completely upon doping.

The size of the conducting islands can be estimated according to the work of Sheng and Abeles¹⁵

$$w' = \frac{kT_0}{4eE_0} \quad (9)$$

Here w' denotes the average width of the conducting grain plus the insulating barrier. The value of w' at different dedoping levels can be found in Table I. Quite surprisingly it is found that w' increases from 42 to 63 Å as the sample gets dedoped. In the redoped 11-layer sample Eq. (9) gives 106 Å. Another way to estimate w' is to measure the field strength E_t at which the conductivity has dropped by a factor of 2 from the value in the Ohmic region.¹⁵ The island size is then $w' = kT/eE_t$. In the dedoped, the moderately dedoped, and the doped states of the 25-layer sample we get $w' = 66, 58, \text{ and } 40 \text{ Å}$ at 80, 77, and 54 K, respectively, which are in good agreement with the values in Table I. Furthermore, E_t decreases as temperature drops as predicted by the model.

The conducting island growth is clearly too large an increase to be solely due to a growing tunneling barrier width because the tunneling probability decreases rapidly

over few tens of angstroms. The fact that the largest island size was measured in a redoped sample suggests that the growth could be due to PF₆⁻ molecules that have been deactivated (HPF₆) by capturing a hydrogen atom from the carbon chain or from a water molecule, but remain inside the conducting islands. They are no longer bound to the polymer carbon chain by a Coulombic attraction, so they are likely to reside further away from the backbone. Dedoped material becomes partly soluble,⁸ which indicates that interchain forces weaken. All this could result in a growth or swelling of the conducting islands of PHT. Redoped and dedoped samples would thus contain considerable amounts of inactive dopants. These speculations do not seem unreasonable, but let us first proceed further in this discussion of dedoped films before drawing any conclusions about the increasing size of conducting islands.

The values of T^* need to be corrected in dedoped samples in order to maintain a good fit of the electric-field dependence of conductivity. Similar but smaller corrections were needed in the measurements of granular metals.¹⁵ Since T_0 could be measured accurately it would mean that the sample temperature had risen. This is, however, very unlikely since the current densities were highest in the measurements of the doped state, in which case no corrections of T^* were necessary. The reason for these corrections has to lie somewhere else and they could perhaps reflect the contribution of the increasing resistance of the conducting islands to the transport properties of charging-energy-limited tunneling.

The original treatment of Sheng and Abeles¹⁵ requires a correlation between grain size and grain separation, and it can be questioned whether this assumption holds in conducting polymers, especially if the tunneling occurs through barriers formed by polymer side chains. The latter is supported by Sato's²⁹ study of electrochemically synthesized poly(3-alkylthiophenes) with PF₆⁻ acting as dopant. The results showed increasing conductivity with decreasing alkyl-chain length. The field-effect mobility and the conductivity have been observed to be larger also in undoped spin cast films of poly(3-alkylthiophenes) with shorter side chains.⁹ Despite some opposing theoretical considerations³⁰ concerning the fractional temperature dependence of conductivity in granular metals, our results here are clearly proportional to $\exp(T^{-1/2})$ and they show very close resemblance to the data of granular metals or cermets where a correlation between grain size and separation is believed to exist. In fact, Sheng³¹ later derived the same temperature dependence by using the critical path method which enabled him to relax the correlation assumption between charging energies and the tunneling distance.

The cermet sample in Ref. 15 with parameters closest to our data at the doped state is 44 vol% Ni in SiO₂ ($kT_0 = 0.34 \text{ eV}$, $E_0 = 0.22 \text{ MV/cm}$, $\sigma_0 = 30 \text{ S/cm}$, $\sigma_\infty(0) = 1 \times 10^{-2} \text{ S/cm}$, $w' = 60 \text{ Å}$). This is a high volume percentage in the transition region between dielectric and metallic regimes. The average distance between grains was determined to be 10 Å, which in our case gives a PHT island size of 32 Å. At lower volume percentages the conductivity level of cermets is naturally

decreased, but in contrast to results here the grain size decreases. This suggests that there is a fundamental difference between our dedoped samples and cermets in the dielectric regime, so that no correlation exists between the PHT island size and their separation. Furthermore, an island size of only 32 Å in the doped state cannot be formed by an aggregation of a great number of PHT molecules, since the average chain length is 108 repeat units giving an average molecule length of about 400 Å. This raises a question whether we are in fact measuring charge transfer between molecules through barriers formed by alkyl side chains. The side chain length is 7–8 Å, which is in agreement with the previous estimate of 10 Å for the barrier width if we assume that the side chains of neighboring molecules are partly interdigitated.

The picture of neighboring polymer chains being separated by alkyl side chains is supported by recent structural studies on poly(3-alkylthiophenes).^{32,33} X-ray diffraction from the semicrystalline regions of the polymer has revealed a layered structure where the polymer chains are stacked on top of each other. The alkyl side chains act as spacers between these stacks. Doping the polymer with iodine³⁴ induces slight expansions and contractions between the stacks, which cannot account for the large changes in conductivity if a tunneling process through the interstack space is assumed.

According to the theory of charging-energy-limited tunneling the temperature dependence of σ_∞ manifests the effect of phonon-assisted tunneling. The motion of charge carriers is quantized within the conducting island and thus a phonon emission or absorption may be required in the tunneling process. The probability of phonon-assisted tunneling increases with temperature and leads to a temperature-dependent σ_∞ . When kT is of the order of the average energy-level separation, a saturation of σ_∞ is expected. Figure 14 shows that such a saturation is indeed observed in the doped state starting at around 35 K. The average energy level separation δ is³⁵

$$\delta = \frac{8E_F}{\pi d^3 n} \quad (10)$$

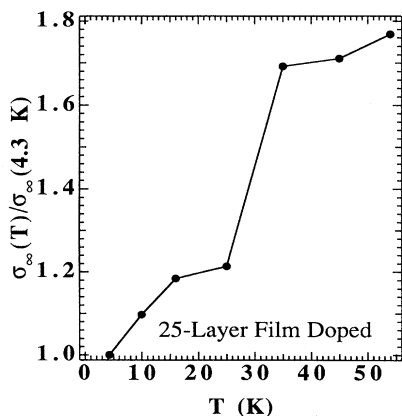


FIG. 14. Relative value of the parameter σ_∞ as a function of temperature in a doped 25-layer sample.

where n is the conduction electron density, E_F the Fermi level, and d the conducting island size. Using the values $\delta \approx kT = 3$ meV, $d = 32$ Å, and $E_F = 5$ eV (Ref. 24) we get $n \approx 1 \times 10^{23} \text{ cm}^{-3}$. This is the density of free charge carriers (holes) inside the conducting islands and it is of the same order as the conduction electron density in metals. As the sample becomes dedoped σ_∞ increases with temperature, but the possible saturation occurs above the temperature range of the measurements. This indicates a decreasing charge-carrier density as both δ and d increase. As discussed earlier, the field-effect measurements (Fig. 3) also show the decrease in conductivity being associated with a decreasing number of charge carriers, but not so much with degrading mobility. These considerations support the tempting speculation of conducting islands being formed by the polymer backbones and separated by alkyl side chains. The conductivity decrease would thus be due to an increase in the resistance (average energy-level separation) within the conducting islands, but it would not be primarily caused by a growing tunneling distance. The increasing average size of conducting islands with dedoping could then be caused by the decreasing density of conducting segments of the polymer backbones. In other words, before tunneling takes place the charge carriers will have to traverse on the average a longer distance along the chain in order to find the next sufficiently conducting part of a neighboring carbon chain.

C. Comparison with free-standing films

All the electrical properties of doped LB films of PHT and 3ODOP discussed so far were reproducible in free-standing films of doped PHT. This is not too surprising since the mole ratio of PHT and the matrix material is high and most of 3ODOP is extracted away during doping. The “quality” of the data obtained from the LB films is better than from free-standing films. This can be partly due to the more sophisticated electrode configuration used with LB films, but it also reflects an electrically more homogeneous material that is very well suited for charge-transport studies.

The temperature dependence of the conductivity in Fig. 11 suggests that the conduction mechanism is the same whether NOPF₆ or FeCl₃ is used as dopant. Charging-energy-limited tunneling has also been observed in FeCl₃-doped polymer blends of poly(3-octylthiophene) and ethylenevinylacetate, where only 10 wt. % of the conductive polymer was used.³⁶ The conducting island size was estimated to be around 100 Å. Hence doping seems to result in the same conduction mechanism in a variety of compositions of poly(3-alkylthiophenes). Moreover, the conducting island size seems to be of the same order (less than 100 Å), as required by the model.

We are unaware of any quantitative model describing the effect of pressure on charging-energy-limited tunneling, but at least qualitatively the behavior in Fig. 13 seems to be correct: as pressure is increased the conductive islands are forced closer to each other and the tunneling barrier width decreases resulting in a drop in resis-

tivity. In the simplest case of elastic tunneling the resistance depends on the tunneling distance D exponentially, $\ln R \propto D$. If the strain is linearly related to the stress (pressure), then $d(\ln R)/dP$ should be constant. As seen in Fig. 13, this is not exactly the case, although there are some linear parts in the curve.

D. Conductivity close to the breakdown field

The behavior of the resistivity close to the breakdown field was shown in Fig. 9. The data points recorded right before the breakdown are replotted in Fig. 15 where a straight line corresponds to a fit to the field-emission theory of Fowler-Nordheim,^{37,38}

$$J = 1.54 \times 10^{-6} E^2 \Phi^{-1} \times \exp[-6.83 \times 10^7 \Phi^{3/2} E^{-1} (m^*/m)^{1/2}], \quad (11)$$

where J is the current density (in A/cm²), Φ is the potential barrier height (in eV), m^*/m is the average effective mass ratio of electrons in the conduction band of the insulating barrier, and E is expressed in V/cm. At high fields the behavior of Eq. (11) is essentially the same as Eq. (3) since the exponent is the dominant variable. It is therefore not easy to distinguish between these two models. However, the proportionality constant is expected to be larger than E_0 in charging-energy-limited tunneling. In our sample the slope of Fig. 9 switches to a value that is larger than E_0 (Table I) by a factor of 17.

Field emission from the Fermi level of the conducting islands to the conduction band of the insulating barrier is expected when the voltage drop across the barrier becomes comparable to the barrier height. In our case the voltage across the electrodes is about 250 V, the distance 5 μm , and the island size about 100 \AA (Table I). Because the voltage drop across the conducting islands is negligible, we have a minimum of 500 tunneling barriers in a single percolation path. This means that $\Phi = 0.5$ eV is the upper limit for the average barrier height. This value would correspond to the situation when the conduction path leads straight through the polymer. Because of the extremely high electric field, tunneling parallel to the field

lines is expected to be favored and the actual barrier height could be close to the above estimate. Using $\Phi = 0.5$ eV and the slope from Fig. 15 in Eq. (11) gives then $m^*/m = 0.97$. Thus the magnitude of the effect is physically acceptable and indicates true Fowler-Nordheim tunneling. It has been previously observed in Si-SiO₂-Al/Mg structures^{38,39} with effective-mass ratios being usually too small ($m^*/m = 0.39-0.48$) compared to the values obtained from current versus temperature measurements ($m^*/m = 0.96$).

The data fit Eq. (11) well, but due to the close proximity to the breakdown, the range of this behavior is not very large. We were not able to check the dependence of Fig. 15 with voltage pulses, and therefore heating effects cannot be completely excluded. However, even higher current densities (see Fig. 7) were sustained in other samples without any signs of joule heating in current transport. Because high current densities cannot be driven through polymers, probably the only way to observe this switching to Fowler-Nordheim tunneling is to use highly dedoped samples at low temperatures.

Knowing the estimate for the barrier height we can further calculate some characteristic values for the tunneling process. We shall first calculate the current density in a single tunneling junction. With 250-V bias and 500 barriers in series we get $E_B = 5$ MV/cm for the electric field across the tunneling barrier if a tunneling width of 10 \AA is assumed. This is a high value, being only a factor of 2 smaller than the dielectric strength of SiO₂. The voltage drop across the junction is 0.5 eV, which indeed shows that the electrons are about to surmount the potential barrier leading to the observed sample breakdown. A substitution of E_B , Φ , and m^*/m into Eq. (11) gives $J_B = 6.6 \times 10^{-11}$ A/ \AA^2 . When this is compared with the total current flowing through the sample at the onset of Fowler-Nordheim tunneling ($j_{\text{tot}} = 10$ μA) we get $j_{\text{tot}}/J_B = 1.5 \times 10^5$ \AA^2 for the combined cross-sectional area of all the conducting pathways through the sample. This is 7.5×10^{-7} times smaller than the total cross-sectional area of the film (2×10^{-5} cm²). The area of a single tunneling barrier cannot be extracted from these calculations, but if we assume it to be of the order of 100 \AA^2 , there would be about 10^3 percolation paths through the sample.

V. CONCLUSIONS

The electrical properties of undoped LB films of PHT and 3ODOP were discussed within the framework of variable-range hopping. However, the possibility of the applicability of the intersoliton hopping model was not excluded. Doping results in a dramatic increase in charge-carrier mobility and the transport properties change. The conduction mechanism in NOPF₆-doped LB films of PHT and free-standing films of the same material was found to be well described by the theory of charging-energy-limited tunneling between conducting islands. The results indicate an increase in the average size of the conducting islands from about 30 to 50 \AA as the material becomes dedoped. The conducting islands were suggested to be formed by parts of conjugated polymer chains which are separated by alkyl side chains. An esti-

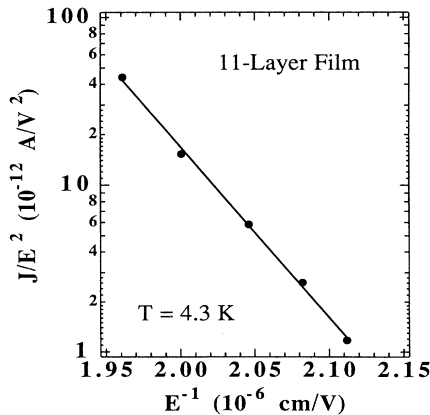


FIG. 15. J/E^2 vs inverse electric field at 4.3 K in a redoped and dedoped (three cycles of doping and dedoping) sample of 11 layers before the breakdown.

mate of about $1 \times 10^{23} \text{ cm}^{-3}$ for the charge-carrier density along a highly doped polymer chain was given on the basis of high-electric-field measurements. At very high electric fields a possible switching to Fowler-Nordheim tunneling was observed. To our knowledge this is the first time Fowler-Nordheim tunneling has been observed in organic materials or granular metals.

ACKNOWLEDGMENTS

The contribution of Yading Wang to the material preparation and doping is gratefully acknowledged. We

thank Dr. Enid Sichel for useful discussions. We are grateful to Dr. Henrik Stubb, Dr. Pekka Kuivalainen, and Jari Paloheimo for reading through the manuscript and providing us with the FET substrates. Financial support from the National Science Foundation, the Finnish Academy of Sciences, and the Technical Research Center of Finland is acknowledged. One of us (E.P.) acknowledges grants from Tekniikan Edistämissäätiö, Neste Oy, A. Kordelin, and O. Öflund foundations. J.D.H. and J.S.B. were supported by National Science Foundation Grant No. 88-18510.

- *Visiting from the Technical Research Centre of Finland, Semiconductor Laboratory, 02150 Espoo, Finland.
- ¹S. Kivelson and A. J. Epstein, *Phys. Rev. B* **29**, 3336 (1984).
- ²E. K. Sichel, M. Knowles, M. Rubner, and J. Georger, Jr., *Phys. Rev. B* **25**, 5574 (1982).
- ³P. Sheng, *Phys. Rev. B* **21**, 2180 (1979).
- ⁴Y. W. Park, A. J. Heeger, M. A. Druy, and A. G. MacDiarmid, *J. Chem. Phys.* **73**, 946 (1980).
- ⁵A. J. Heeger and A. G. MacDiarmid, *Mol. Cryst. Liq. Cryst.* **77**, 1 (1981).
- ⁶R. R. Chance, J. L. Bredas, and R. Silbey, *Phys. Rev. B* **29**, 4491 (1984).
- ⁷I. Watanabe, K. Hong, and M. F. Rubner, *Langmuir* **6**, 1164 (1990).
- ⁸Y. Wang and M. Rubner, *Synth. Met.* **39**, 153 (1990).
- ⁹J. Paloheimo, E. Punkka, H. Stubb, and P. Kuivalainen, in *Lower Dimensional Systems and Molecular Devices*, Vol. XX of *NATO Advanced Study Institute Series B: Physics*, edited by R. M. Metzger (Plenum, New York, in press).
- ¹⁰R. Guertin and S. Bloom (private communication).
- ¹¹J. Paloheimo, E. Punkka, P. Kuivalainen, H. Stubb, and P. Yli-Lahti, *Acta Polytech. Scand. Electr. Eng. Ser.* **64**, 178 (1989).
- ¹²S. M. Sze, *Physics of Semiconductor Devices* (Wiley, New York, 1981).
- ¹³N. F. Mott and E. A. Davis, *Electronic Processes in Non-Crystalline Materials*, 2nd ed. (Clarendon, Oxford, 1979).
- ¹⁴A. L. Efros and B. I. Shklovskii, *J. Phys. C* **8**, L49 (1975).
- ¹⁵P. Sheng and B. Abeles, *Phys. Rev. Lett.* **31**, 44 (1973); B. Abeles, P. Sheng, M. D. Coutts, and Y. Arie, *Adv. Phys.* **24**, 407 (1975).
- ¹⁶N. Apsley and H. P. Hughes, *Philos. Mag.* **31**, 1327 (1975).
- ¹⁷A. D. Yoffe and R. T. Phillips, in *Disordered Semiconductors*, edited by M. A. Kastner, G. A. Thomas, and S. R. Ovshinsky (Plenum, New York, 1987).
- ¹⁸M. Pollak and M. Riess, *J. Phys. C* **9**, 2339 (1976).
- ¹⁹M. Van der Meer, R. Schuchardt, and R. Keiper, *Phys. Status*

- Solidi* **110**, 571 (1982).
- ²⁰R. Colson and P. Nagels, *J. Non-Cryst. Solids* **35**, 129, (1980).
- ²¹J. Paloheimo, P. Kuivalainen, H. Stubb, E. Vuorimaa, and P. Yli-Lahti, *Appl. Phys. Lett.* **56**, 1157 (1990).
- ²²H. Tomozawa, D. Braun, S. D. Phillips, A. J. Heeger, and H. Kroemer, *Synth. Met.* **22**, 63 (1987).
- ²³E. Punkka and M. F. Rubner, *Synth. Met.* (to be published).
- ²⁴G. Gustafsson, M. Sundberg, O. Inganäs, and C. Svensson, *J. Mol. Electron.* **6**, 105 (1990).
- ²⁵S. Kivelson, *Phys. Rev. Lett.* **46**, 1344 (1981); *Phys. Rev. B* **25**, 3798 (1982).
- ²⁶A. J. Heeger and A. G. MacDiarmid, *Mol. Cryst. Liq. Cryst.* **77**, 1 (1981).
- ²⁷P. Kuivalainen, H. Stubb, H. Isotalo, P. Yli-Lahti, and C. Holmström, *Phys. Rev. B* **31**, 7900 (1985).
- ²⁸A. J. Epstein, H. Rommelman, M. Abkowitz, and H. W. Gibson, *Mol. Cryst. Liq. Cryst.* **77**, 81 (1981).
- ²⁹M.-A. Sato, S. Tanaka, and K. Kaeriyama, *Synth. Met.* **18**, 229 (1987).
- ³⁰C. J. Adkins, *J. Phys. C* **15**, 7143 (1982).
- ³¹P. Sheng and J. Klafter, *Phys. Rev. B* **27**, 2583 (1983).
- ³²G. Gustafsson, O. Inganäs, H. Österholm, and J. Laakso, *Polymer* (to be published).
- ³³M. J. Winokur, D. Spiegel, Y. Kim, S. Hotta, and A. J. Heeger, *Synth. Met.* **28**, C419 (1989).
- ³⁴M. J. Winokur, P. Wamsley, J. Moulton, P. Smith, and A. J. Heeger (unpublished).
- ³⁵R. Kubo, *J. Phys. Soc. Jpn.* **17**, 975 (1962).
- ³⁶E. Punkka, J. Laakso, H. Stubb, and P. Kuivalainen, *Phys. Rev. B* **41**, 5914 (1990).
- ³⁷R. H. Fowler and L. W. Nordheim, *Proc. R. Soc. London Ser. A* **119**, 173 (1928).
- ³⁸E. H. Snow, *Solid State Commun.* **5**, 813 (1967); M. Lenzlinger and E. H. Snow, *J. Appl. Phys.* **40**, 278 (1969).
- ³⁹J. G. Simmons, *DC Conduction in Thin Films* (Mills and Boon, London, 1971).